Carrier transport in amorphous silicon-based thin-film transistors studied by spin-dependent transport

Genshiro Kawachi
Hitachi Research Laboratory, Hitachi Ltd., Hitachi, Ibaraki 319-12, Japan

Carlos F. O. Graeff, Martin S. Brandt, and Martin Stutzmann
Walter Schottky Institut, Technische Universität München, Garching, 85748, Germany
(Received 16 October 1995; revised manuscript received 11 April 1996)

Carrier transport processes in hydrogenated amorphous silicon-based thin-film transistors (*a*-Si:H TFT's) are investigated by spin-dependent transport (SDT). Spin-dependent photoconductivity (SDPC) signals arising from less than 10^6 spins in a small transistor are detected with an adequate signal-to-noise ratio. SDPC measurements reveal two different limiting steps for the light-induced leakage current in TFT's depending on the gate voltage: bulk recombination in undoped *a*-Si:H and recombination near the source junction. Also, the leakage current mechanism under high source-drain fields is identified by SDT measurements in the dark as electron hopping via defect states located at the interface between undoped *a*-Si:H and the passivation silicon nitride layer. Both silicon dangling bonds and nitrogen dangling bonds seem to be involved in the electron hopping process. At temperatures below 100 K, spin-dependent hopping of electrons in conduction-band tail states is observed. The change of the dominant transport path from extended state conduction to variable range hopping conduction with decreasing temperature is confirmed by SDT measurements.
[S0163-1829(96)00436-5]

I. INTRODUCTION

Spin-dependent transport (SDT) is a powerful method for investigating carrier transport processes in semiconductors. The major advantages of this technique are (i) enhanced detection sensitivity, (ii) *in situ* detection of paramagnetic defects under normal operating conditions, (iii) the capability of providing information about the microscopic structure of paramagnetic defects as in conventional electron-spin resonance (ESR). There are a number of reports on the observation of ESR-induced conductivity changes in crystalline silicon,[1] crystalline *p-n* junctions,[2–4] silicon/silicon dioxide interfaces,[5,6] polycrystalline silicon,[7,8] and amorphous silicon.[9,10] In hydrogenated amorphous silicon (*a*-Si:H), Dersch, Schweitzer, and Stuke[11] have identified two elementary processes in carrier recombination by spin-dependent photoconductivity (SDPC). Recent progress in this field has been reported by Lips, Schütte, and Fuhs[12] and Brandt and Stutzmann[13] showing that all paramagnetic states that give ESR signals are also detectable by SDT. These studies demonstrate the high potential of this method for material characterization. Although it seems to be intriguing to apply SDT for characterization of active devices, such attempts are quite limited so far.[14] In this paper, we report on the results of the application of SDT to amorphous silicon-based field-effect transistors that are now key components for various microelectronics applications.

Thin-film transistors based on hydrogenated amorphous silicon (*a*-Si TFT's) are one of the most important applications in amorphous silicon technology. They have already been adopted as switching elements in active-matrix liquid-crystal displays[15] and various image sensing devices.[16] In spite of the rapid growth of their industrial importance, however, still many important issues remain to be investigated. It is well known that localized electronic states arising from structural disorder and structural defects in *a*-Si:H adversely affect the device performance.[17] Thus, understanding the nature of localized states is essential for designing and improving these devices. SDT is considered as a suitable means for studying these localized states in TFT's, not only because of its high detection sensitivity which allows us to obtain information from a small number of paramagnetic states contained in small devices, but due to the fact that it directly observes the interactions between charge carriers and localized states under normal operation.

In addition to the technological importance described above, *a*-Si TFT's can also be used as a tool to study spin physics in *a*-Si:H. Using three terminal metal-insulator-semiconductor devices, one can vary a variety of physical parameters, such as carrier density or internal fields over a wide range. This fact opens the possibility of observing resonance phenomena which cannot be detected in a simple gap-cell structure with Ohmic contacts. This paper reports detailed results of SDT in *a*-Si TFT's aiming to study carrier transport processes in these devices. After describing experimental procedures, results on spin-dependent photoconductivity (SDPC) in *a*-Si TFT's are shown in Sec. III. The carrier recombination kinetics in *a*-Si:H TFT's is discussed. In Sec. IV, the observation of spin-dependent hopping in the leakage and forward currents are described. The leakage current mechanism and carrier transport at low temperatures are discussed on the basis of these observations.

II. EXPERIMENTAL DETAIL

The sample used in this study were state of the art inverted-staggered TFT's with silicon nitride (Si_3N_4) as the gate insulator described elsewhere in more detail.[18] A cross-

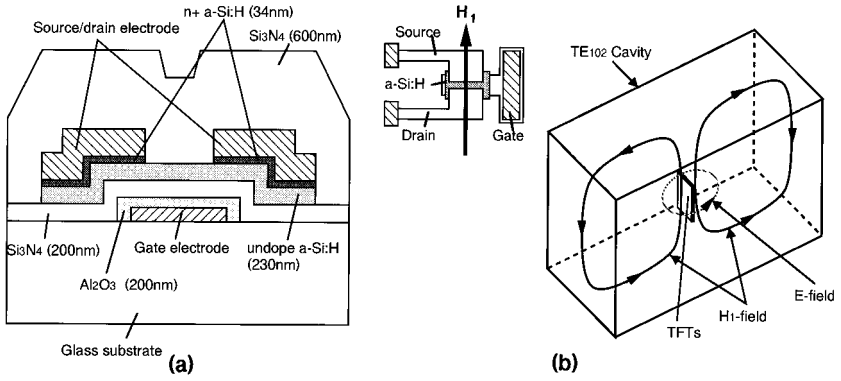

FIG. 1. (a) Cross-sectional view of the *a*-Si TFT. (b) Placement of TFT in the TE_{102} cavity and representation of field patterns.

sectional drawing of the TFT is shown in Fig. 1(a). The bottom (gate) electrode consists of Al covered with a Al_2O_3 film with thickness of 180 nm formed by anodic oxidation. Si_3N_4 (200 nm), undoped *a*-Si:H (220 nm), and n^+ *a*-Si:H (34 nm) were deposited consecutively in a multichamber plasma enhanced chemical vapor deposition reactor. The Si_3N_4 film for the gate dielectric was deposited at 300° C from a mixed gas of SiH_4 and NH_3 with a flow-rate ratio of NH_3 to SiH_4 of 6. The undoped *a*-Si:H film for the active layer was deposited from pure SiH_4 at 250 ° C. The n^+ *a*-Si:H film for the source and drain contacts was deposited at 250 °C from a mixed gas of SiH_4, H_2, and PH_3 with a flow-rate ratio of PH_3 to SiH_4 of 0.01. A layered electrode consisting of Cr and Al was deposited on the n^+ *a*-Si:H by sputtering, and patterned into the source and drain contacts. The n^+ *a*-Si:H between the source and drain contacts was etched off by reactive ion etching. Finally, the device was covered with silicon nitride film deposited at 230 °C. The channel width/length (W/L) ratio of the TFT's was varied from 10/10 μm to 830/10 μm. The typical effective mobility and threshold voltage of TFT's were 0.3 cm^2/V s and 1 V, respectively.

A standard *X*-band (9 Ghz) ESR spectrometer (Bruker ESP300) was used for SDT experiments. The sample was amounted on the top of a quartz tube, and placed in the middle of the TE_{102} cavity where the microwave magnetic field is maximum. TFT's were placed so that the source-drain current direction was in parallel with the microwave magnetic field H_1 in the cavity as shown in Fig. 1(b). For spin-dependent photoconductivity (SDPC) measurements, TFT's were illuminated from the source-drain side with a tungsten lamp using a RG650 cutoff filter. The spin-dependent change of the source-drain current was detected by a lock-in amplifier as a function of the external magnetic field. A magnetic-field modulation technique was employed to obtain the first derivative of the resonance spectra. The modulation frequency was varied from 177 Hz to 5 kHz. The modulation amplitude was kept at 6 G throughout all measurements. The measurement temperature was varied from 5 to 295 K using a He gas-flow cryostat.

III. SPIN-DEPENDENT PHOTOCONDUCTIVITY IN *a*-SI TFT'S

A. Detection sensitivity

For the observation of ESR-induced photoconductivity changes, it is essential that at least two paramagnetic states are involved in the recombination process. Since the field-effect transistor is a unipolar device, it has to be illuminated to inject minority carriers. In Fig. 2, typical transfer curves of the TFT in the dark and under illumination are shown. The photocurrent obtained after subtracting the dark current is also indicated in the figure. The leakage current at negative gate voltage is increased by several orders due to the photogenerated carriers. The SDPC signal was detectable over the entire range of the gate bias; however, the signal is getting smaller as the gate voltage increases.[19] The dependence of the resonance spectra on the gate bias will be discussed in Sec. III B, in connection with the recombination kinetics.

As mentioned previously, one of the strengths of SDT is its enhanced detection sensitivity. A measurement using small TFT's can be a good test of the achievable sensitivity. Figure 3 compares SDPC spectra obtained from three TFT's with different W/L ratios. The peak-to-peak width ΔH_{pp} of the resonance line increases slightly with increasing W. It is found that the line broadening is caused by microwave field enhancement in the TFT due to the strong coupling between the microwave field and the TFT structure. The detailed analysis of the field enhancement effect in TFT's will be described elsewhere.[20] The signal-to-noise (S/N) ratio deteriorates as the W/L ratio decreases, because the photocurrent decreases with decreasing W/L. Since the SDPC signal intensity is proportional to the photocurrent which scales with the W/L ratio, also the S/N ratio scales with the W/L ratio. Nevertheless, it is still possible to detect a signal with an adequate S/N ratio even in the smallest device studied which

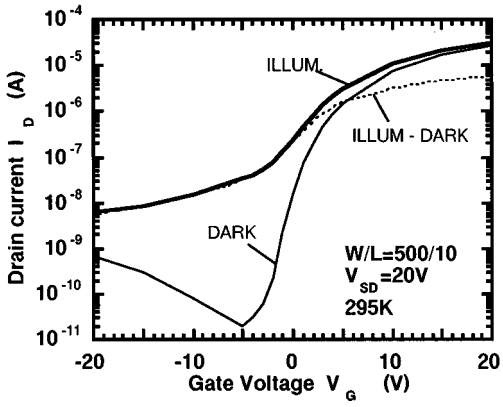

FIG. 2. Transfer characteristics of the *a*-Si TFT at 295 K. The broken curve indicates the photocurrent after subtracting the dark current.

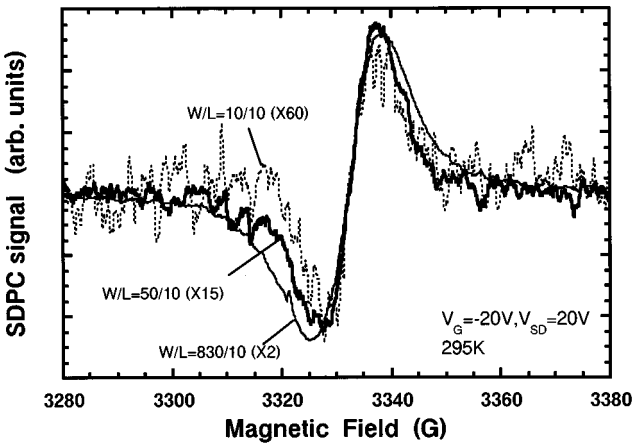

FIG. 3. Spin-dependent photoconductivity spectra in a-Si TFT's with different channel widths/lengths (W/L). The spectra were taken at $V_G=-20$ V and $V_{SD}=20$ V.

has an active area of $10\times 10\ \mu m^2$. Assuming that the defect density in undoped a-Si:H film is 10^{16} cm^{-3}, the absolute number of defects in this device is estimated to be 10^5. Thus, we could gain the detection sensitivity by at least a factor of 10^7 compared to conventional ESR where the detection limit for dangling bonds in a-Si:H is 10^{12} spins. It is not difficult to reduce the device size to less than $1\times 1\mu m^2$ using state of the art semiconductor technology. Thus, one can expect to observe a signal from less than 10^4 spins by SDT in such devices. The above results demonstrate the applicability of SDT for exploring defects and carrier transport in small structures.

B. Recombination processes in a-Si TFT's

Now let us turn to details of carrier recombination processes in TFT's. The SDPC spectra in TFT's depends on the gate voltage as indicated in Fig. 4. With increasing negative gate voltage, a gradual shift of the g factor to larger values, together with a change in the spectral weight of the resonance towards lower magnetic fields is observed. The line shape does not show a remarkable change when the gate voltage is increased from -4.5 to 10 V. The line-shape change suggests a change in the dominant recombination steps with gate bias. Dersch, Schweitzer, and Stuke[11] have proposed a two-step recombination model in a-Si:H on the basis of the SDPC observation as follows: (1) tunneling of electrons trapped in the conduction-band tail states to neutral dangling bonds, (2) hopping of holes in the valence-band tail states which enhances the capture of holes by negatively charged dangling bonds. The first step gives rise to a resonance line with $g=2.0050$ and $\Delta H_{pp}=9$ G (e-db line), and the latter step gives rise to a resonance line with $g=2.01$ and $\Delta H_{pp}=20$ G (h line). The change in the line shape shown in Fig. 4, thus, suggests an increase in the hole component with decreasing negative gate voltage. In fact, phase-shift analysis, as described by Dersch, Schweitzer, and Stuke,[11] reveals that the spectrum for $V_G=-4.5$ V can be decomposed into two components: a narrow line with $g=2.0053$ and a broad line with $g=2.0093$. Thus, we can conclude that the hopping of holes in the valence-band tail states becomes a rate limiting process for the photo current at small negative gate voltages. It is interesting to note that the measurement temperature for our TFT is 295 K because the h line in SDPC spectra has been detectable only below 200 K in the previous reports.[11,21] To understand the implication of the results shown in Fig. 4, we have to consider the carrier dynamics in field-effect transistors. As already shown in Fig. 2, the photocurrent increases with V_G as well as the dark current despite a constant excitation intensity. This implies the presence of a current amplification mechanism. This can be understood in terms of the parasitic bipolar effect in field-effect transistors as follows: At $V_G=4.5$ V, where the transistor is in the subthreshold regime, an electron accumulation layer is already formed at the a-Si:H/Si_3N_4 interface. One can see a n-i-n bipolar transistor consisting of n^+a-Si:H/undoped a-Si:H/electron channel as illustrated in Fig. 5(a). The n^+a-Si:H, undoped a-Si:H and the surface accumulation layer can be considered as the emitter, base, and collector of the parasitic bipolar transistor, respectively.

Photogenerated electrons are swept away by the source-drain field across the electron channel. Photogenerated holes, on the other hand, drift towards the source and are blocked by the potential barrier at the source function. Holes trapped in the gap states produce a positive space charge and reduce

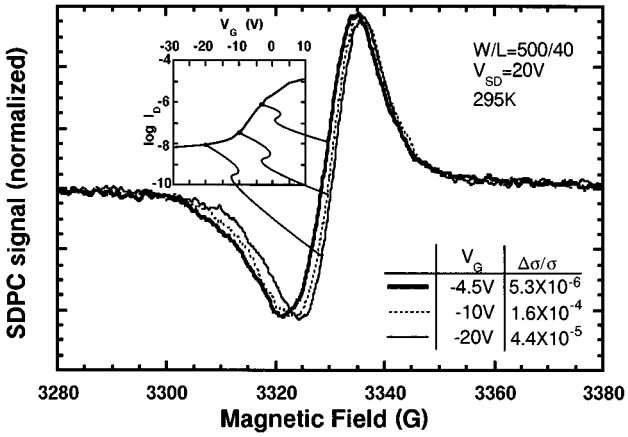

FIG. 4. SDPC spectra at various gate voltages. Measurements were carried out at the points on the transfer characteristics shown in the inset.

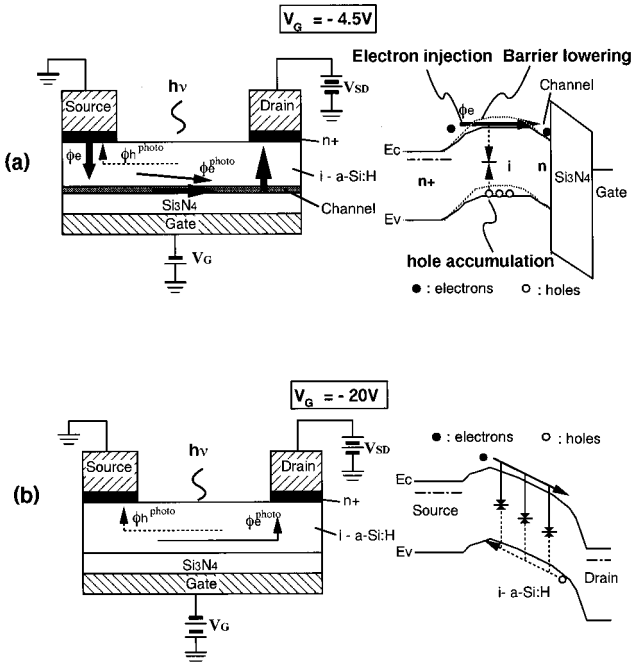

FIG. 5. Schematic diagrams of the photoleakage current mechanism and potential profiles in the device: (a) small negative gate bias; (b) large negative gate bias.

the potential barrier of the source junction, resulting in an increase of electron injection from the source electrode. The recombination occurs mainly at the n^+/i source junction between the injected electron and trapped holes. Recombination between the injected electrons and trapped holes reduces the amount of the positive space charge, thereby reducing the electron injection. Since the electron current is strongly influenced by the amount of trapped holes, the spin-dependent hopping of holes which enhance electron-hole recombination can be a rate limiting step of the drain current, resulting in the appearance of the hole resonance even at room temperature. The recombination kinetics does not change at positive gate voltages where the TFT is in the *on* state because the parasitic bipolar transistor is still existing. Thus, the line shape does not change when the V_G is increased up to 10 V. On the other hand, when the gate voltage is becoming more negative, the bipolar effect vanishes because there is no electron channel. The injected electrons recombine with holes in the undoped *a*-Si:H layer as in the case of standard photoconductivity gap cells with Ohmic contacts. The current limiting process is recombination in the entire *a*-Si:H layer as indicated in Fig. 5(b). Therefore, the hole component disappears and the resonance signal shows quite a similar line shape to those reported so far for thin-film photoconductivity.

The parasitic bipolar action has been observed in short-channel silicon on insulator transistors where the hole current is generated by impact ionization in the drain depletion region.[22,23] Although we lack direct evidence for the occurrence of the bipolar action in our *a*-Si TFT's, it seems to be a reasonable model for understanding why hole hopping becomes the current limiting step in the *n*-channel device.

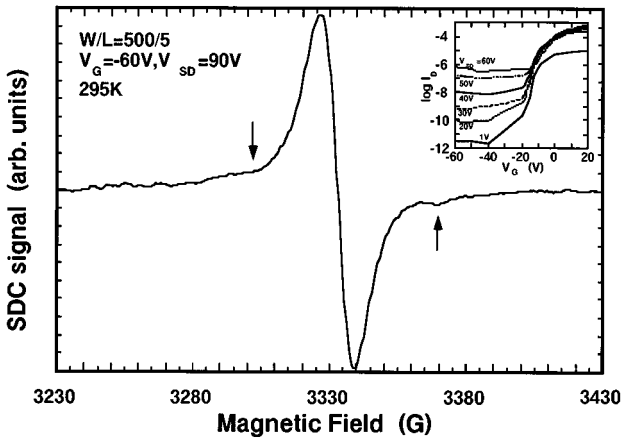

FIG. 6. Spin-dependent conductivity spectra in the dark current at high negative gate bias and large source-drain field. Typical leakage current characteristics at various source-drain voltages are shown in the inset. Note that the resonance signal is enhancing (positive derivative of the absorption signal).

IV. SPIN-DEPENDENT CONDUCTIVITY IN *a*-SI TFT'S

A. Leakage current in *a*-Si TFT's at high electric fields

The leakage current is one of the most important quantities for Si TFT's used in imaging devices, because it has a great influence on the image quality of these devices. Thus, it is important to investigate the leakage current mechanism in TFT's from a microscopic point of view using SDT. In the previous section, we have investigated the rate limiting process of the photogenerated leakage current. In this section, another leakage current path in *a*-Si TFT's observed at high electric fields is studied.

A SDT resonance signal is found at large source-drain voltages and large negative gate voltages. The signal is observable without light excitation at room temperature. The signal is enhancing, meaning that the current increases at resonance. A typical spectrum measured at a microwave power of 200 mW is shown in Fig. 6. The signal has a wide-based Lorentzian line shape with the peak-to-peak width $\Delta H_{\rm pp}$ of 20 G and the zero-crossing *g* factor of 2.0054. The signal amplitude $\Delta\sigma/\sigma$ reaches up to 2.9×10^{-3}, which is much larger than that of the SDPC signal shown in the previous section. Note that the line shape is affected by the enhanced microwave field in the TFT. The leakage current characteristics of the TFT for various source-drain voltages $V_{\rm SD}$ are indicated in the inset of Fig. 6. The leakage current depends slightly on the gate voltage, whereas it depends nearly exponentially on $V_{\rm SD}$. The SDC signal amplitude, on the other hand, depends both on $V_{\rm SD}$ and V_G as shown in Fig. 7. Another interesting feature of the spectrum is the appearance of a hyperfine structure at the position indicated by arrows in Fig. 6. The separation between the two hyperfine peaks is about 70 G. Recently, an ESR spectrum with two satellite peaks having a splitting of 70 G in stoichiometric or nitrogen-rich silicon nitride films has been reported and identified as nitrogen dangling bond (N-dB).[24,25] Noting the similarity of the line shape between the results of Ref. 24 and Fig. 6, it is likely that defects in silicon nitride films are involved in the transport path giving rise to the leakage cur-

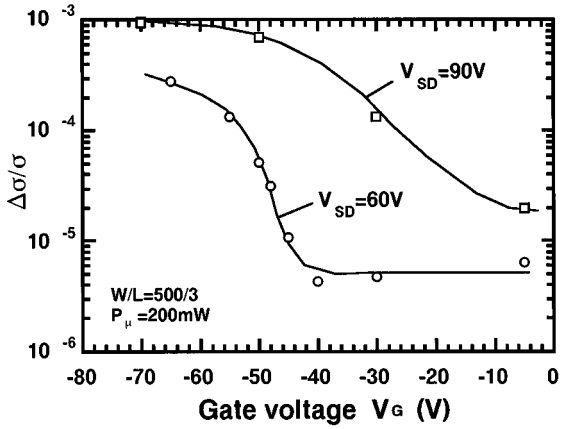

FIG. 7. SDC signal amplitude as a function of the gate bias for different source-drain voltages.

rent. ^{29}Si can be another candidate responsible for the observed hyperfine structure because a pair of hyperfine lines observed in the ESR spectra of Si dangling bonds also has a splitting of about 70 G.[26] However, the ratio of the hyperfine structure to the entire spectrum of Fig. 6 is estimated to be 15%, and is much larger than 4.7% which corresponds to the natural abundance of ^{29}Si. Thus, we can rule out this possibility.

The signal amplitude I^{SDC} and peak-to-peak linewidth ΔH_{pp} are plotted as a function of the microwave power P_μ in Fig. 8. The power dependence shows quite distinctive features. The signal amplitude I^{SDC} increases as $I^{\mathrm{SDC}} \propto P_\mu^{0.5}$ below 10 mW. Above 10 mW, the power dependence changes to $I^{\mathrm{SDC}} \propto P_\mu$. Corresponding to the above, ΔH_{pp} shows a linear dependence on $P_\mu^{0.5}$ below 10 mw, and tends to saturate above 10 mW. The zero-crossing g factor does not change with P_μ. This saturation behavior clearly indicates that the observed resonance line consists of signals arising from different types of paramagnetic centers. The first component, which is dominant below $P_\mu = 10$ mW, is already affected by the saturational broadening effect. The second component, which is dominant above $P_\mu = 10$ mW, does not experience the saturational broadening even at the maximum microwave power (200 mW), implying that this second component has a much broader linewidth than the first component. Judging from the g value (2.0054), it is likely that the first component originates from Si dangling bonds. It is reasonable to ascribe the second component to a N-db, because the line shape, which has two satellite peaks with a splitting of 70 G and the lack of saturation are quite similar to those of N-db.[24,25]

Then how can defects in silicon nitride films be involved in the carrier transport? The fact that the resonance is an enhancing signal suggests the transport path to be due to spin-dependent hopping via defect states. There are three possible current paths which may involve defects in silicon nitride films: (i) electron or hole hopping through the gate dielectric film (gate leakage current), (ii) hole hopping via defects located at the interface between the gate insulator and a-Si:H films, and (iii) electron hopping via defects located at the interface between the a-Si:H film and the passivation silicon nitride film. The first possibility is unlikely because no stable leakage current that allow us to measure such a

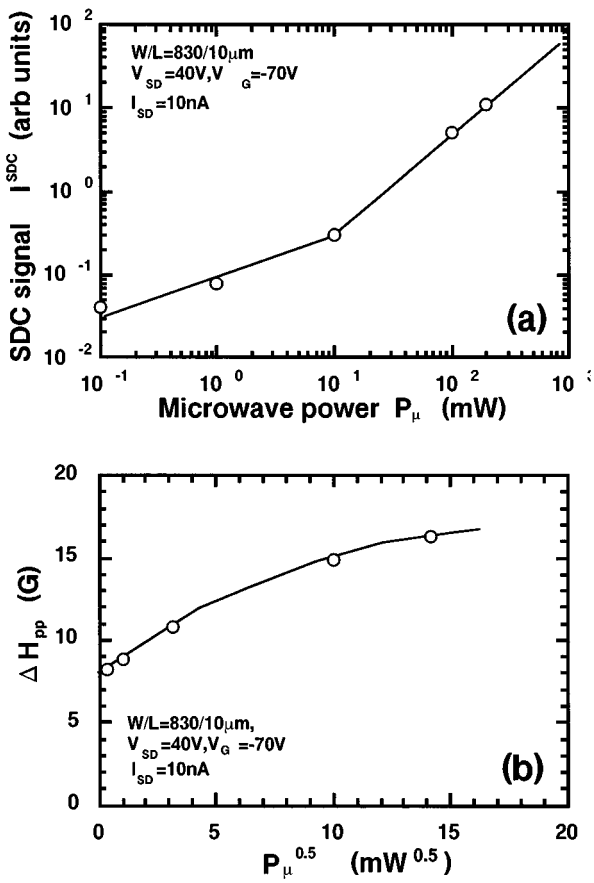

FIG. 8. (a) SDC signal amplitude as a function of microwave power. The signal amplitudes were corrected by multiplying with the square of the peak-to-peak linewidths. (b) The peak-to-peak linewidth as a function of the square root of the microwave power.

large signal has been detected in our TFT's. It is possible to distinguish between the second and third possibilities by taking into account the dependence of the leakage current and SDC signal intensity on the gate bias. As shown in Fig. 7, $\Delta\sigma/\sigma$ increases steeply with increasing negative gate bias V_G above a certain value, while the leakage current increases only slightly with negative gate bias increases. Therefore, the vertical field induced by the gate bias does influence the spin dependence of the transport path, but not the current itself. Taking into account this fact, we can rule out mechanism (ii). For occurrence of the hole conduction, holes have to be injected from the drain junction by tunneling.[27] The tunneling probability of holes will strongly depend on the electric field in the drain depletion region and, therefore, depends strongly on the vertical field because the drain field in inverted staggered TFT's is parallel to this vertical field. Thus, we would expect an exponential dependence of the leakage current on the gate voltage, as observed in polycrystalline Si TFT's.[27] This is not the case for our TFT's. Consequently, we can conclude that the dominant conduction path which gives to the SDT signal is electron hopping via defect states at the backinterface between the a-Si:H film and passivation silicon nitride film. For negative gate voltages, the strong vertical field pushes electrons towards the backinterface thereby injecting electrons into the interface defects which act as hopping sites. The rapid increase of $\Delta\sigma/\sigma$ with in-

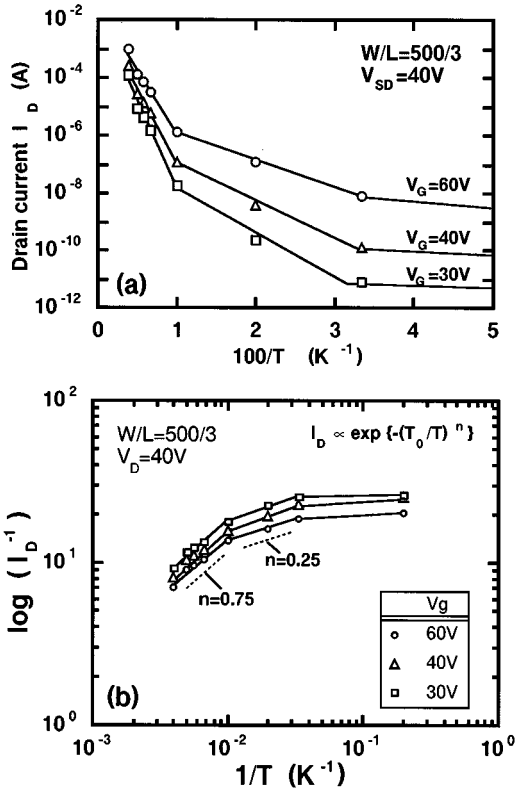

FIG. 9. Temperature dependence of the drain current of a-Si TFT's for various gate voltages: (a) I_D vs 100/T plots, (b) $\log_{10}\{\log_{10}(I_D^{-1})\}$ vs $\log_{10}(T^{-1})$ plots.

creasing negative gate bias may be explained by this injection. The occurrence of such a conduction at the back interface is possible because the passivation silicon nitride film is deposited at a relatively low temperature (230 °C) with a NH_3 rich gas composition ($NH_3/SiH_4=6$) and, thus may have a high defect density. The microscopic mechanism of this conduction process is unclear at the present stage. Further studies on transport at the a-Si:H-Si_3N_4 interfaces would be necessary to clarify this point. However, it is clear from above observation that the leakage current in a-Si:H TFT's at high electric fields is due to hopping conduction at the back interface, confirming the fact that understanding and careful control of electronic properties of interfaces have special importance for improving device performance.

B. Electron transport in surface accumulation layer at low temperatures

Hopping conduction in the band-tail states has been observed in n-type and p-type a-Si:H, using SDT.[13,28] The field-effect transistor is considered an ideal system for investigating band-tail conduction, because the Fermi-level position can be readily varied over a wide range by changing the gate bias. Using a transistor instead of doped materials, one can explore shallow tail states located very close to the mobility edge. In this section, the observations by SDT of electron hopping at the Si_3N_4/a-Si:H interface at low temperatures are described.

Figure 9(a) shows the temperature dependence of the drain current of the a-Si TFT for various gate voltages. Two

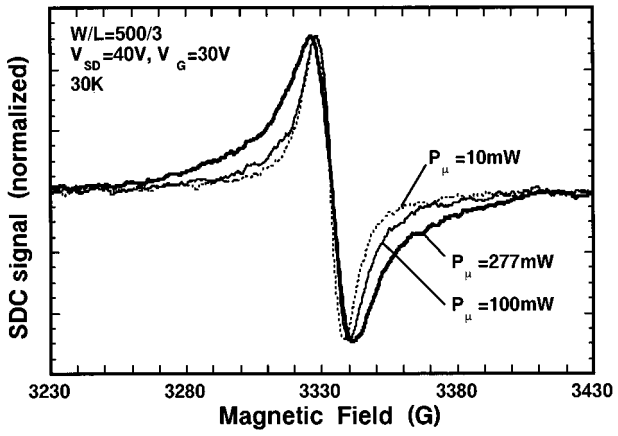

FIG. 10. SDC spectra in the forward current measured at 30 K for various microwave powers. Note that the spectra were broadened by enhanced microwave field in TFT's.

kinks seen at $T=100$ and 30 K suggest changes of the transport mechanism at these temperatures. Lustig *et al.*[29] have reported the temperature dependence of the drain current in a-Si TFT's between 80 and 400 K, and found two distinct transport mechanisms: conduction in extended states observed above 260 K and variable range hopping conduction in conduction-band tail states between 80 and 260 K. The variable range hopping conduction is characterized by the temperature dependence represented by Mott's formula[30] as

$$\sigma=\sigma_0\exp(-(T_0/T)^n), \tag{1}$$

where T_0 is a constant depending on the density of states at the Fermi energy and the electron localization length. The exponent n is equal to $\frac{1}{4}$ and $\frac{1}{3}$ for three- and two-dimensional systems, respectively. In general, it is difficult to determine the power of the temperature because $\log_{10}\sigma$ vs T^{-n} plots give good linear fits to the data for a relatively wide range of n. Here, we use a different approach. In Fig. 9(b), $\log_{10}\{(\log_{10}I_D^{-1})\}$ is plotted as a function of $\log_{10}(T^{-1})$ for various gate voltages. The slope of the data give the values of n. Three temperature regimes shown in Fig. 9(a) are characterized by values of n as follows: (i) $n=0.75$ for $250>T>100$ K, (ii) $n=0.25$–0.3 for $100>T>30$ K, and (iii) $n=0$ for 30 K $>T$. Judging from these values of n, the temperature regime where the variable range hopping dominates electron conduction is between 100 and 30 K. Above 100 K, variable range hopping and thermally activated conduction in extended states seem to be coexisting, because n takes a value between 0.25 and 1. Below 30 K, electron conduction is dominated by hopping without phonon assistance.

Applying spin-dependent transport to this problem, we note that SDC signals are observed below 100 K at relatively large positive gate voltages. Figure 10 shows SDC spectra measured at 30 K. The signal is an enhancing line (the current increases at the resonance) with a g factor of 2.0040. The g factor was independent of the microwave power, measurement temperature, and gate voltage. The peak-to-peak width ΔH_{pp} increases slightly with increasing microwave power; however, it does not change with the measuring temperature and gate voltage. At large positive gate voltages, the

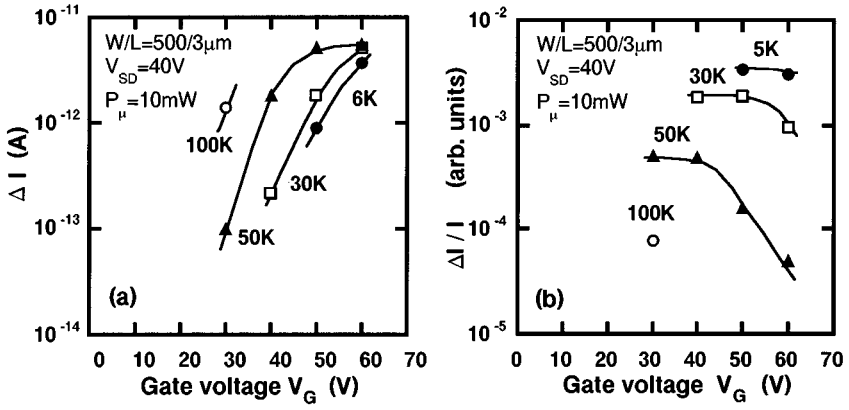

FIG. 11. (a) Maximum change in current at resonance field as a function of the gate bias at various temperatures, (b) normalized signal amplitude as a function of the gate bias at various temperatures.

Fermi energy at the a:Si:H/Si_3N_4 interface must be moved into the conduction-band tail states. Thus, it is reasonable to conclude that the enhancing SDC signal comes from spin-dependent electron hopping at tail states.

Figures 11(a) and 11(b) show the change in the drain current at resonance ΔI and the normalized signal amplitude, $\Delta I/I$, as a function of gate voltage for various measurement temperatures. The absolute change ΔI increases with increasing V_G or T while $\Delta I/I$ decreases with increasing V_G or T, suggesting that the spin-independent current component increases more rapidly with V_G or T than the spin-dependent current does. This result can be understood by taking into account the increasing delocalization of electrons. When the gate voltage increases, the Fermi level is moved close to the mobility edge, resulting in an increase of excitation of localized electrons to extended states. Also increasing temperature enhances delocalization of trapped electrons. In fact, the observation of spin-dependent change in the drain current was almost undetectable above 100 K. Since the conduction by delocalized electrons is most likely spin independent because of their short spin-lattice relaxation time, the spin-dependent current is buried under the spin-independent current. The above results are consistent with the temperature dependence of the current indicated in Fig. 9. The increase of conduction in extended states leads to a change of temperature dependence from $I_D \propto T^{-1/4}$ to $I_D \propto T^{-3/4}$ above 100 K and simultaneously decreases the spin-dependent resonance signal.

V. CONCLUSIONS

Spin-dependent transport has been applied for the investigation of the carrier transport process in a-Si:H-based thin-film transistors. SDPC signals arising from less than 10^6 spins in a small transistor can be detected with an adequate signal-to-noise ratio. Two different current limiting steps under illumination are detected by SDPC measurements. For large negative gate bias, the photoleakage current is determined by bulk recombination in the a-Si:H layer. With decreasing negative gate bias, the occurrence of a parasitic bipolar effect causes recombination near the source junction to become a current limiting process.

Spin-dependent hopping conduction via defects states located at the back interface of TFT's is identified by SDC signals observed in the leakage current under large source-drain fields. Both Si dangling bonds and N dangling bonds located at the backinterface seem to be involved in the hopping process.

Spin-dependent hopping of electrons in conduction-band tail states is detected by a SDC measurement at low temperatures. The change with decreasing temperature of the dominant transport path from extended state conduction to variable range hopping conduction in tail states is confirmed. These results demonstrate that spin-dependent transport can be applied advantageously for a variety of problems concerning carrier transport in small devices.

ACKNOWLEDGMENTS

The authors would like to thank M. Ishii (Hitachi Ltd.), N. Reinacher, and D. Lanz (Technical University of Munich) for technical assistance. One of the authors (G.K.) would also like to acknowledge Dr. Mr. Nishihara, Dr. K. Miyauchi, Dr. T. Minemura, Y. Nagae, and N. Konishi (Hitachi Ltd.) for their constant encouragement.

[1] D. J. Lepine, Phys. Rev. B **6**, 436 (1972).
[2] I. Solomon, Solid State Commun. **20**, 215 (1976).
[3] M. X. Yan, K. P. Honewood, and B. C. Cavenett, J. Phys. C **19**, L189 (1986).
[4] Z. Kachwalla and D. J. Miller, J. Appl. Phys. **62**, 2848 (1987).
[5] M. A. Jupina and P. M. Lenahan, IEEE Trans. Nucl. Sci. **36**, 1800 (1989).
[6] R. L. Vranch, B. Henderson, and M. Pepper, Appl. Phys. Lett **52**, 1161 (1988).
[7] W. K. Schubert and P. M. Lenahan, Appl. Phys Lett. **43**, 497 (1983).
[8] C. H. Seager, E. L. Venturini, and W. K. Schubert, J. Appl. Phys. **71**, 5059 (1992).
[9] I. Solomon, D. K. Biegelsen, and J. S. Knights, Solid State Commun. **22**, 595 (1977).

[10] N. Kishimoto, K. Morigaki, and K. Maurakami, J. Phys. Soc. Jpn. **50**, 1970 (1981).
[11] H. Dersch, L. Schweitzer, and J. Stuke, Phys. Rev. B **28**, 4678 (1983).
[12] K. Lips, S. Schütte, and W. Fuhs, Philos. Mag. B **65**, 945 (1992).
[13] M. S. Brandt and M. Stutzmann, Phys. Rev. B **43**, 5184 (1991).
[14] K. Lips and W. Fuhs, J. Appl. Phys. **74**, 3993 (1993).
[15] A. J. Snell, K. D. Mackenzie, W. E. Spear, P. G. LeComber, and A. J. Hughes, Apply. Phys. **24**, 357 (1981).
[16] K. Rosan, in *Amorphous and Microcrystalline Semiconductor Devices-Optelectronic Devices*, edited by J. Kanicki (Artech House Inc., Norwood, 1991), p. 241.
[17] M. J. Powell, IEEE Trans. Electron Devices **ED-36**, 2753 (1989).
[18] H. Yamamoto, H. Matsumaru, K. Shirahashi, M. Nakatani, A. Sasano, N. Konishi, K. Tsutsui, and T. Tsukada, in *Proceedings of International Electron Device Meeting* (IEEE, San Francisco, 1990), p. 851.
[19] C. F. O. Graeff, M. S. Brandt, M. Stutzmann, and M. J. Powell, Phys. Rev. B **52**, 4680 (1995).
[20] G. Kawachi, C. F. O. Graeff, M. S. Brandt, and M. Stutzmann (unpublished).
[21] M. S. Brandt and M. Stutzmann, J. Non-Cryst. Solids **164–166**, 547 (1993).
[22] M. Hack and A. G. Lewis, IEEE Trans. Electron Device Lett. **EDL-12**, 203 (1991).
[23] J. G. Fossum, R. Sundaresan, and M. Matloubian, IEEE Trans. Electron Device Lett. **EDL-8**, 544 (1987).
[24] W. L. Warren, P. M. Lenahan, and S. E. Curry, Phys. Rev. Lett. **65**, 207 (1990).
[25] H. Yan, M. Kumeda, N. Ishii, and T. Shimizu, Jpn. J. Appl. Phys. **32**, 876 (1993).
[26] D. K. Biegelsen and M. Stutzmann, Phys. Rev. B **33**, 3006 (1986).
[27] J. Fossum, A. Ortiz-Conde, H. Shichijo, and S. Banerjee, IEEE Trans. Electron Devices **ED-41**, 1878 (1985).
[28] H. Dersch and L. Schweitzer, Philos. Mag. B **50**, 397 (1984).
[29] N. Lustig. J. Kanicki, R. Wisnieff, and J. Griffith, in *Amorphous Silicon Technology*, edited by A. Madan, M. J. Thompson, P. C. Taylor, P. G. LeComber, and Y. Hamakawa, MRS Symposia Proceedings No. 118 (Materials Research Society, San Francisco, 1988), p. 267.
[30] N. F. Mott, J. Non-Cryst. Solids **1**, 1 (1968).